Cardiac Deformation from Electro-Anatomical Mapping Data: Application to Scar Characterization

A.R. Porras[1], G. Piella[1], Oscar Cámara[1], E. Silva[2], D. Andreu[2], A. Berruezo[2], and A.F. Frangi[1,3]

[1] CISTIB - Universitat Pompeu i Fabra, CIBER-BBN, Barcelona, Spain
[2] Hospital Clinic, IDIBAPS, Universitat de Barcelona, Barcelona, Spain
[3] Institucio Catalana de Recerca i Estudis Avanats (ICREA), Barcelona, Spain

Abstract. We propose in this paper a new way of calculating an endocardial end-systolic deformation parameter from electro-anatomical data acquired intra-operatively during electrophysiology interventions. The estimated parameter is then used to study deformation in regions with different viability properties: scar, border zone and normal myocardial tissue. These regions are defined based on electrophysiological data acquired with a contact mapping system, specifically with the bipolar voltage maps and a set of routinely used thresholds. The obtained results when applying our methodology on a set of 8 cases show statistically significant differences between the average deformation values of the scar, border zone and normal myocardial tissue areas, thus demonstrating the feasibility of detecting changes in deformation between normal and non-healthy tissue from electro-anatomical maps. Nevertheless, although low deformation regions more often correspond to non-healthy tissue, deformation is not an accurate indicator of viability abnormalities.

1 Introduction

Scar presence and its characteristics play a fundamental role in several cardiac pathologies. Most of ventricular tachycardias (VTs) present in patients with ischemia are produced by a re-entrance mechanism associated to the presence of scars [1], which are composed by areas of dense fibrosis that cause a conduction block, as well as other areas of fibrosis where it is possible to find myocardial cells with low-speed conduction [2]. Catheter ablation is an option for recurrent VT treatment. To improve its applicability and effectiveness, a detailed knowledge of the ventricular scar and border zone is required. In addition, it has been proven that scar location, morphology and physiology play an essential role on Cardiac Resynchronization Therapy (CRT) planning [3].

Several methods have been used to identify the region affected by the scar. Delay-Enhancement Magnetic Resonance Imaging (DE-MRI) allows quantifying the area with fibrosis and its level of transmurality, making it possible to detect and assess the myocardial viability. However, these images are obtained prior to the intervention, being its use for guidance during the ablation procedure hampered.

D.N. Metaxas and L. Axel (Eds.): FIMH 2011, LNCS 6666, pp. 47–54, 2011.

Therefore, electro-anatomical mapping is the most used way to locate the area to be treated. It basically consists in introducing one catheter into the ventricle and, with a tracking system, recording the position and electrical activity of different points on the endocardium wall. Since reduced endocardial voltage indicates electrically abnormal tissue, scar, border zone and normal tissue can be delimited according to their electrical activity. This approach has the advantage that it is an intra-procedure method and the same catheter can be used to perform the ablation. However, some studies have concluded that it is hard to establish absolute values that can be used to differentiate between scar, border zone and normal tissue for all patients [4]. Moreover, spatial resolution in this kind of procedures is usually very low.

To complement electrical information, mechanical properties can also be analyzed. This is actually possible with current electro-anatomical mapping systems since trajectories for each acquired point are recorded, allowing motion of the heart wall to be estimated and hence providing information on cardiac mechanics [5]. During the last few years, the idea of extracting motion/deformation from electro-anatomical mapping systems has started to be exploited, as it is the case of NOGA system (Biologics Delivery Systems Group, Cordis Corporation, Irwindale CA, USA), which provides a linear local shortening index [6] as an indicator of local contraction of the myocardium.

The main goal of this paper is to propose a new way to calculate deformation from CARTO XP (Biosense Webster, Haifa, Israel) electro-anatomical data [7] and to analyze how tissue viability defined by electrical data behaves in terms of deformation. We focus on deformation analysis rather than motion, since passive non-deforming regions can show motion due to tethering to adjacent regions and overall heart motion [8]. The deformation parameter is computed with a strain-like equation after point filtering, but projecting all points onto an estimation of the plane tangent to the endocardial surface.

2 Cardiac Deformation Estimation

CARTO XP is an electrophysiological contact mapping system mostly used for anatomical guidance of ablation procedures. The obtained electro-anatomical maps consist of electrical signals (recorded at 1kHz) and position data of the catheter (recorded at 100Hz) over 2.5s.

2.1 Data Pre-processing

Before the deformation analysis, some of the tracked points were removed to filter out possible acquisition errors, i.e. the catheter sliding over the endocardial wall or the contact of the catheter on the wall being unstable. For this study, points were removed according to the following two criteria:

1. Points whose positions in two consecutive cardiac cycles are too far away. We filtered those points whose distances between two consecutive end diastoles were greater than 10mm, in a similar way as proposed in [9]. End-diastole is

taken as reference because CARTO XP synchronizes all points according to the R-peak of the electro-cardiogram (end-diastole), so it is a good reference.
2. Isolated points that did not have any point closer than 25mm, since it makes local deformation estimation not reliable enough. This threshold has been chosen regarding to the mean distance between the points.

Furthermore, since motion and electrical data are sampled with different rates, motion data have been linearly interpolated.

2.2 Deformation Estimation

The following step in our proposed methodology is the deformation analysis, once position data have been resampled. For each analyzed point, the Endocardial End-Systolic Deformation (EESD) can be estimated from its Euclidean distance to the closest points in space by using the following expression:

$$EESD = \frac{L_{ED} - L_{ES}}{L_{ED}} \tag{1}$$

where L_{ED} is the distance between points at end-diastole, and L_{ES} represents the same distance at end-systole.

According to Eq. 1, areas with high deformation should ideally have a higher value (close to 1) for EESD than areas with low deformation (which should be close to 0), as long as the distance between points in end-systole is smaller than in end-diastole (which should be the normal situation).

This approach cannot, however, be directly applied over electro-anatomical data because each point is acquired in different time instants. Even though the mapping system synchronizes all points to the R-peak of the electro-cardiogram, there is a lack of synchronization away from this instant that is intrinsic to the acquisition procedure. This is illustrated in Fig. 1, where we can see two simplified examples of endocardial wall displacement between diastolic and systolic phases. In the ideal case, when there are no synchronization errors between neighboring points away from the trigger point, L_{ES} is shorter than L_{ED}. On the other hand, when two adjacent points are not in the same time instant of the cardiac cycle, L_{ES} can be equal or larger than L_{ED}.

In Fig. 1, we can appreciate that most of the error is introduced in the radial direction. Thus, part of the synchronization problem could be eliminated if we filter motion in this direction. This can be done by projecting the length vectors in a plane tangent to the endocardial wall surface.

However, we do not have enough data to accurately calculate such a tangent plane. Thus, we have estimated this plane by finding the spatial center of all points at end-diastole, so that a vector from one point to this center is a very coarse approximation to the radial direction. Since this direction is normal to the tangent plane, we just have to project point distances onto this plane and calculate the deformation parameter in Eq. 1 by using these projections rather than real distances, as illustrated in Fig. 2.

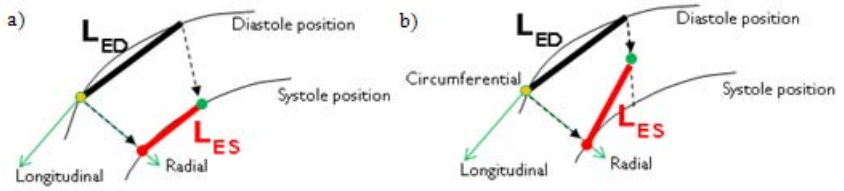

Fig. 1. a) Ideal situation for points acquired with electro-anatomical mapping systems, where L_{ES} is shorter than L_{ED}. b) Situation where for a certain acquisition time, two points are not in the same time instant of the cardiac cycle, so L_{ES} can be equal or larger than L_{ED}.

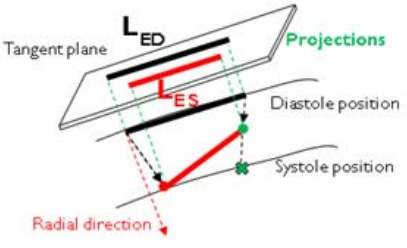

Fig. 2. Projection of end diastolic and end systolic distances onto the tangent plane. When projecting, L_{ES} is smaller or equal than L_{ED} in most cases.

2.3 Statistical Analysis

Data are expressed as mean ± standard deviation. Comparisons between all data were done using a Student's t-test and results were considered statistically significant at a p value lower than 0.05.

Moreover, a ROC analysis has been carried out to find out whether EESD can discriminate between normal and un-healthy tissue.

2.4 Clinical Data

For the deformation analysis, we have used electro-anatomical maps from 4 VT patients and 4 CRT patients (age 72.25 ± 4.71 years). The maps were acquired with CARTO XP and had an average of 380 ± 219 points (range 83 - 548 points) for VT patients and 76 ± 35 points (range 49 - 124) for CRT patients.

3 Results

Before the deformation analysis, 27.9 ± 11.6% points were filtered. Afterwards, EESD maps have been compared between scar, border zone and normal myocardial tissue. Tissue type has been defined according to their electrical activity, which is the currently used gold standard [10]. Hence, points whose maximum

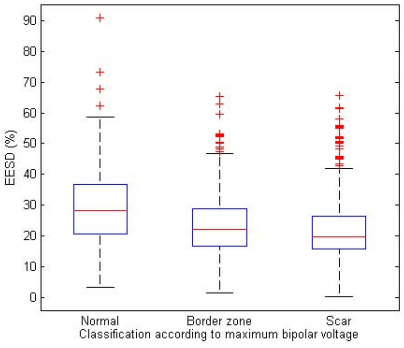

Fig. 3. Box plots showing the EESD distribution for all points. For each box, the central mark represents the median, the boxes represent the first and third quartiles and the crosses represent outliers.

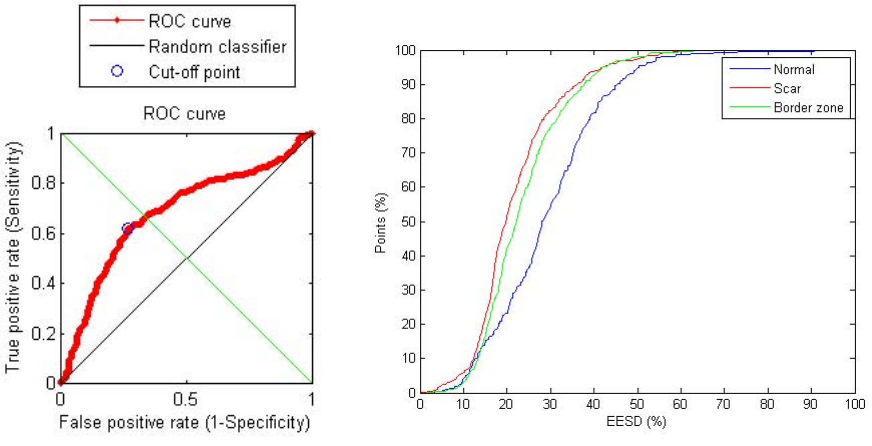

Fig. 4. On the left, a ROC curve when classifying normal from un-healthy tissue is represented. On the right, the cumulated percentage of points as function of deformation value for scar, border zone and normal tissue is shown.

bipolar voltage is lower than 0.5mV are considered as scar, while points with maximum bipolar voltage between 0.5mV and 1.5mV are defined as border zone.

Normal tissue showed a larger mean deformation than the border zone ($29 \pm 13\%$ vs. $24 \pm 10\%, p \leq 0.05$) and scar regions ($29 \pm 13\%$ vs. $22 \pm 10\%, p \leq 0.05$), while scar regions showed lower mean deformation than border zone ($22 \pm 10\%$ vs. $24 \pm 10\%, p \leq 0.05$). Fig. 3 shows the box plots of the EESD distribution for the points from all patients.

The ROC analysis for the EESD is shown in Fig. 4, where the obtained cut-off value that best discriminates un-healthy from normal tissue is 25.8%. The cumulated percentage of points for each deformation value is also represented.

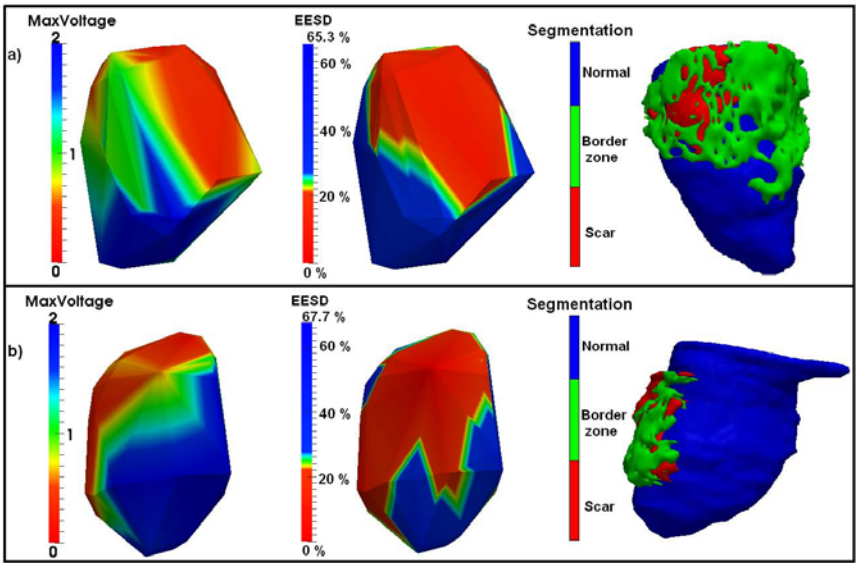

Fig. 5. Reconstruction of the left ventricle for two patients (a and b) from CARTO XP data. For each patient, maximum bipolar voltages (scale in mV) are shown on the left, EESD values are shown on the middle and manual segmentation from DE-MRI on the right. For the voltage maps, regions in red correspond to scar and regions in blue are related to normal tissue. For EESD maps, colors range from red (low EESD value) to blue (high EESD value).

Finally, in Fig. 5, a view of two patient's left ventricle reconstruction (with Delaunay triangulation) from CARTO XP data is shown, where both electrical and EESD data are represented. For visual comparison, a manual segmentation of scar, border zone and normal tissue from DE-MRI performed by experts has also been included.

4 Discussion

The obtained results suggest that points in normal myocardial tissue have a higher deformation than points in the scar. Moreover, points on the border zone seem to have a higher deformation than scar, but lower than normal tissue.

However, although the differences in EESD between the three kind of tissue are statistically significant, one can appreciate in Fig. 3 that there is a considerable overlap in their ranges. This is in agreement with previous studies using the NOGA system [11].

The ROC analysis shown in Fig. 4 suggests that, for the optimal EESD cut-off value, specificity and sensitivity are low. Moreover, 25% of normal points have a lower value for EESD than the cut-off value, and 29% of points in scar have a higher value. Hence, we can conclude that discrimination based only in the EESD would not be reliable with the data analyzed in this paper.

Under the hypothesis that regions with scar have a reduced deformation when compared to normal tissue, there is a considerable mismatching (as shown in Fig. 5) with respect to tissue classification based on electrical activity. This fact was partially expected, because deformation and electrical activity show two different and complementary characteristics of endocardial tissue. It is important to point out that the classification based on electrical activity has been done using absolute thresholds for bipolar voltages.

EESD computation is very dependent on the quality and proximity of the acquired points and thus, we are very conditioned by the acquisition method. The underlying problem is that, beside the measurement error of the tracking system, every point is acquired independently, so there is a general lack of synchronization that introduces an error. Furthermore, when acquiring a point, the catheter usually slides over the endocardial surface, as can easily be appreciated when visualizing its trajectory. Since deformation is very sensitive to small changes in motion between every two points, it is very affected by all these errors. It would be possible to filter out some of the artifacts present in the recorded motion signal if their nature was known. For example, the error introduced by respiration motion could be removed by filtering the frequencies associated to it, or the lack of synchronization between points could be overcome by applying signal re-synchronization methods. Nevertheless, the most important artifact is produced by the catheter sliding over the endocardial and it would be very difficult to automatically detect and remove it.

5 Conclusions

In this paper, we have proposed a new way for estimating deformation from electro-anatomical data acquired with a widely used contact mapping system. We found that, even though there is a statistically significant difference between the mean of EESD for scar, border zone and normal tissue, low deformation is not always an indicator of low electrical activity. Dually, high deformation does not always correspond to normal electrical activity.

These results are limited by the sparse spatial information and the various sources of error derived from the acquisition procedure. Hence, it would be necessary to use data from other intra-operative modalities to improve on the reliability of the deformation computation.

Future work includes a co-registration of CARTO data to DE-MRI segmentation to quantify its correspondence with the EESD proposed.

Aknowledgements

This research has been partially funded by the Industrial and Technological Development Center (CDTI) under the CENIT-cvREMOD program. The work by O. Camara is supported by the Spanish Ministry of Science and Innovation through the Ramon y Cajal Program.

References

[1] Svenson, W.G.: Ventricular scars and ventricular tachycardia. Transactions of the American Clinical and Climatological Association 120, 403–412 (2009)
[2] de Bakker, J., van Capelle, F., Janse, M., Tasseron, S., Vermeulen, J., de Jonge, N., Lahpor, J.: Slow conduction in the infarcted human heart. 'zigzag' course of activation. Circulation 88(3), 915–926 (1993)
[3] Duckett, S.G., Ginks, M., Shetty, A.K., Knowles, B.R., Totman, J.J., Chiribiri, A., Ma, Y.L., Razavi, R., Schaeffter, T., Carr-White, G., Rhode, K., Rinaldi, C.A.: Realtime fusion of cardiac magnetic resonance imaging and computed tomography venography with x-ray fluoroscopy to aid cardiac resynchronisation therapy implantation in patients with persistent left superior vena cava. Europace (2010)
[4] Botker, H.E., Lassen, J.F., Hermansen, F., Wiggers, H., Sogaard, P., Kim, W.Y., Bottcher, M., Thuesen, L., Pedersen, A.K.: Electromechanical mapping for detection of myocardial viability in patients with ischemic cardiomyopathy. Circulation 103, 1631–1637 (2001)
[5] Camara, O., Oeltze, S., De Craene, M., Sebastian, R., Silva, E., Tamborero, D., Mont, L., Sitges, M., Bijnens, B.H., Frangi, A.F.: Cardiac motion estimation from intracardiac electrical mapping data: Identifying a septal flash in heart failure. In: Ayache, N., Delingette, H., Sermesant, M. (eds.) FIMH 2009. LNCS, vol. 5528, pp. 21–29. Springer, Heidelberg (2009)
[6] Psaltis, P., Worthley, S.: Endoventricular electromechanical mapping the diagnostic and therapeutic utility of the noga xp cardiac navigation system. Journal of Cardiovascular Translational Research 2, 48–62 (2009)
[7] Ben-Haim, S., Osadchy, D., Schuster, I., Gepstein, L., Hayam, G., Josephson, M.: Nonfluoroscopic, in vivo navigation and mapping technology. Nature Medicine 2(12), 1393–1395 (1996)
[8] Gorcsan, John, I.: Echocardiographic Strain Imaging for Myocardial Viability: An Improvement Over Visual Assessment? Circulation 112(25), 3820–3822 (2005)
[9] Klemm, H., Ventura, R., Franzen, O., Baldus, S., Mortensen, K., Risius, T., Willems, S.: Simultaneous mapping of activation and motion timing in the healthy and chronically ischemic heart. Heart Rhythm 3(7), 781–788 (2006)
[10] Dickfeld, T., Lei, P., Dilsizian, V., Jeudy, J., Dong, J., Voudouris, A., Peters, R., Saba, M., Shekhar, R., Shorofsky, S.: Integration of three-dimensional scar maps for ventricular tachycardia ablation with positron emission tomography-computed tomography. JACC: Cardiovascular Imaging 1(1), 73–82 (2008)
[11] Samady, H., Liu, Y., Choi, C., Ragosta, M., Pfau, S., Cleman, M., Powers, E., Kramer, C., Wackers, F., Beller, G., Watson, D.: Electromechanical mapping for detecting myocardial viability and ischemia in patients with severe ischemic cardiomyopathy. The American Journal of Cardiology 91(7), 807–811 (2003)